

pubs.acs.org/accounts Article

N-Arylimide Molecular Balances: A Comprehensive Platform for Studying Aromatic Interactions in Solution

Ping Li, Erik C. Vik, and Ken D. Shimizu*



Cite This: Acc. Chem. Res. 2020, 53, 2705-2714



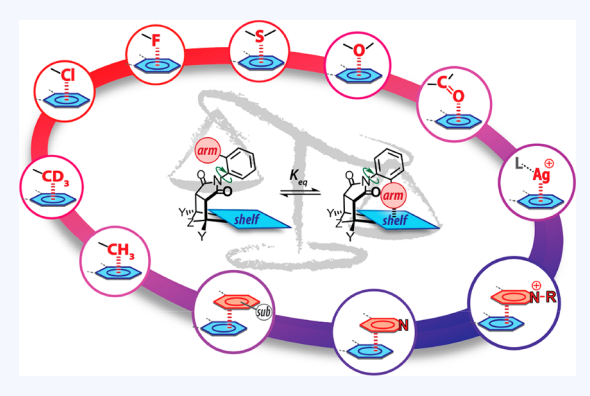
ACCESS

III Metrics & More



3 Supporting Information

CONSPECTUS: Noncovalent interactions of aromatic surfaces play a key role in many biological processes and in determining the properties and utility of synthetic materials, sensors, and catalysts. However, the study of aromatic interactions has been challenging because these interactions are usually very weak and their trends are modulated by many factors such as structural, electronic, steric, and solvent effects. Recently, N-arylimide molecular balances have emerged as highly versatile and effective platforms for studying aromatic interactions in solution. These molecular balances can accurately measure weak noncovalent interactions in solution via their influence on the folded—unfolded conformational equilibrium. The structure (i.e., size, shape, π -conjugation, and substitution) and nature (i.e., element, charge, and polarity) of the π -surfaces and interacting groups can be readily varied, enabling the study of a wide range of aromatic



interactions. These include aromatic stacking, heterocyclic aromatic stacking, and alkyl $-\pi$, chalcogen $-\pi$, silver $-\pi$, halogen $-\pi$, substituent $-\pi$, and solvent $-\pi$ interactions. The ability to measure a diverse array of aromatic interactions within a single model system provides a unique perspective and insights as the interaction energies, stability trends, and solvent effects for different types of interactions can be directly compared. Some broad conclusions that have emerged from this comprehensive analysis include: (1) The strongest aromatic interactions involve groups with positive charges such as pyridinium and metal ions which interact with the electrostatically negative π -face of the aromatic surface via cation $-\pi$ or metal $-\pi$ interactions. Attractive electrostatic interactions can also form between aromatic surfaces and groups with partial positive charges. (2) Electrostatic interactions involving aromatic surfaces can be switched from repulsive to attractive using electron-withdrawing substituents or heterocycles. These electrostatic trends appear to span many types of aromatic interactions involving a polar group interacting with a π -surface such as halogen $-\pi$, chalcogen $-\pi$, and carbonyl $-\pi$. (3) Nonpolar groups form weak but measurable stabilizing interactions with aromatic surfaces in organic solvents due to favorable dispersion and/or solvophobic effects. A good predictor of the interaction strength is provided by the change in solvent-accessible surface area. (4) Solvent effects modulate the aromatic interactions in the forms of solvophobic effects and competitive solvation, which can be modeled using solvent cohesion density and specific solvent—solute interactions.

■ KEY REFERENCES

- Carroll, W. R.; Pellechia, P.; Shimizu, K. D. A Rigid Molecular Balance for Measuring Face-to-Face Arene-Arene Interactions. Org. Lett. 2008, 10, 3547–3550.¹ This was our first publication introducing our molecular balance system and its application to measuring and studying aromatic stacking interactions in solution.
- Hwang, J.; Li, P.; Carroll, W. R.; Smith, M. D.; Pellechia, P. J.; Shimizu, K. D. Additivity of Substituent Effects in Aromatic Stacking Interactions. J. Am. Chem. Soc. 2014, 136, 14060–14067.² This publication highlighted the ability of the N-arylimide balances to experimentally test hypotheses and to develop new predictive models for aromatic interactions.
- Hwang, J.; Li, P.; Smith, M. D.; Shimizu, K. D. Distance-Dependent Attractive and Repulsive Interactions of Bulky Alkyl Groups. Angew. Chem., Int. Ed. 2016, 55,

- 8086–8089.³ This publication demonstrated that aromatic interactions spanning attractive and repulsive interactions can be modeled using a universal model.
- Li, P.; Vik, E. C.; Maier, J. M.; Karki, I.; Strickland, S. M. S.; Umana, J. M.; Smith, M. D.; Pellechia, P. J.; Shimizu, K. D. Electrostatically Driven CO-π Aromatic Interactions. J. Am. Chem. Soc. 2019, 141, 12513–12517.⁴ This publication demonstrated that electronegative atoms and groups can form attractive interactions with aromatic surfaces if the surfaces are sufficiently electron-poor.

Received: August 14, 2020 Published: November 5, 2020





■ INTRODUCTION

Noncovalent interactions of aromatic surfaces play key roles in biological and synthetic structures, catalysts, and processes. 5–8 However, the measurement and study of aromatic interactions have been very challenging. One successful strategy has been to design molecular instruments to measure aromatic interactions via their influence on a conformational equilibrium (Figure 1A). 9,10 Oki 11 and Wilcox 12 pioneered the approach of

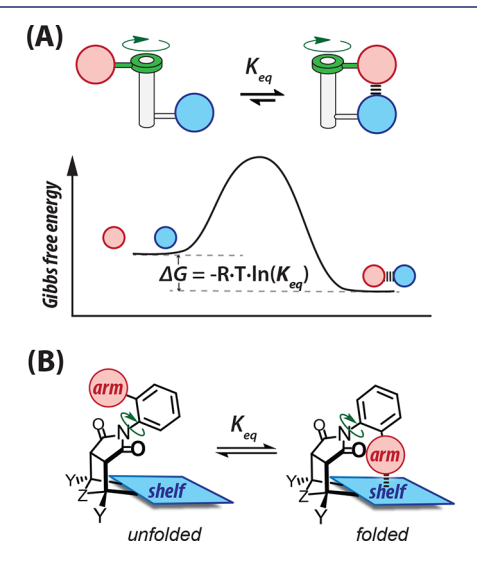


Figure 1. (A) Schematic representation of a molecular balance that measures the noncovalent interactions between two covalently attached surfaces (red and blue) through their influence on a conformational equilibrium. (B) Folded—unfolded equilibrium of *N*-arylimide molecular balances designed to measure the intramolecular arm—shelf interactions in the folded conformer.

designing molecular-scale instruments to measure weak noncovalent interactions via their influence on a conformational equilibrium. Since then, there have been a number of successful molecular balance systems reported in the literature. This article describes the insights and lessons learned in our studies of noncovalent aromatic interactions using the versatile *N*-arylimide molecular balance platform (Figure 1B).

■ N-ARYLIMIDE MOLECULAR BALANCES

In the search for a rigid yet conformationally dynamic framework to study aromatic interactions, we came across the *N*-arylimide rotamers reported by Verma, ¹⁴ Kishikawa, ¹⁵ and Grossman. ¹⁶ The *N*-arylimide molecular balances contain a C_{aryl}-N_{imide} single bond with restricted rotation that connects the interacting arm and aromatic shelf units, leading to the formation of distinct folded and unfolded conformers (Figure 1B). In the folded conformer, the arm unit is held in close proximity to the face of the aromatic shelf by the rigid C-shaped framework. Conversely, in the unfolded conformer, the arm and aromatic shelf are held apart and cannot interact. Thus, the folded-unfolded equilibria can serve as a very sensitive gauge of the strengths of the intramolecular interactions in the folded conformers of these molecular balances.

A key advantage of the N-arylimide balances was the ease of monitoring their conformational equilibria via 1H or ^{19}F NMR at room temperature. Due to the slow rotation of the $C_{aryl}-$

 N_{imide} bond on the NMR time scale, each conformer has a distinct set of resonances that can be integrated to provide an accurate measure of the equilibrium ratio (Figure 2, K_{eq}). K_{eq}

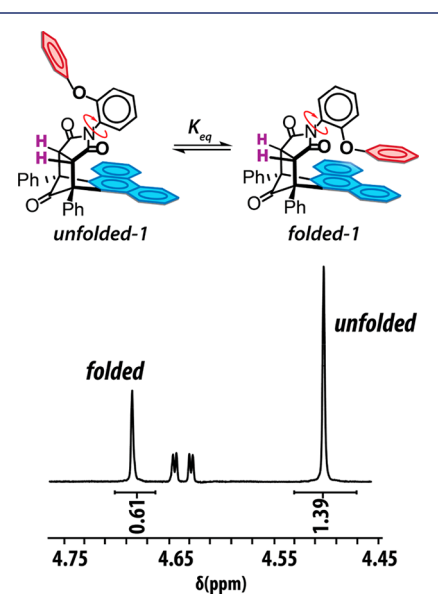


Figure 2. ¹H NMR spectra highlighting the region with the succinimide protons (purple) used to measure the folded/unfolded ratio of N-arylimide molecular balance 1 that was designed to measure the stacking interaction in solution (CDCl₃, 25 °C). Data are from ref

was surprisingly sensitive to small changes in interaction strength due to the logarithmic relationship between the folding energy and $K_{\rm eq}$: $\Delta G = -RT \ln([{\rm folded}]/[{\rm unfolded}])$. For example, a small change in the folding energy ($\Delta\Delta G$) of 0.1 kcal/mol translates to an 18.5% change in the folding ratio ($K_{\rm eq}/K'_{\rm eq}$), which can be very easily and accurately measured by integration of the $^1{\rm H}$ NMR spectra. The folding energies can be measured to an accuracy of ± 0.02 kcal/mol based on an error of 3% in peak ratios. This sensitivity is actually a limitation when studying stronger interactions that tip the equilibrium too far in one direction. Thus, the N-arylimide balances can measure only weaker interactions with an upper limit of ± 2.3 to ± 4.6 kcal/mol, depending on the folding ratios of the control balances (vide infra).

Our initial studies demonstrated the need to "tare" the balances using separate control balances (Figure 3).^{1,17} For example, the equilibrium ratio for balance 1 was less than unity $(K_{eq} = +0.43)$, suggesting that the intramolecular stacking interaction was repulsive and destabilizing. However, when the folding energy for balance 1 was tared using control balance 3 (tare value = +1.39 kcal/mol), the attractive and stabilizing nature of the stacking interaction was evident (-0.90 kcal/ mol) and consistent in magnitude with previous studies. 18,19 A similar analysis of balance 2 measured a slightly stronger stacking interaction energy of -1.07 kcal/mol for the larger pyrene aromatic shelf. Thus, even in this minimal model system, there were significant additional interactions and biases. The folding energies of 1 and 2 were influenced not only by the stacking interaction (Figure 3, broken blue lines) but also by the repulsive interaction between the oxygen linker and π -surface (broken red lines), which was stronger than the attractive interactions of interest. Control balance 4 confirmed that the $O-\pi$ interaction was the predominant bias in this

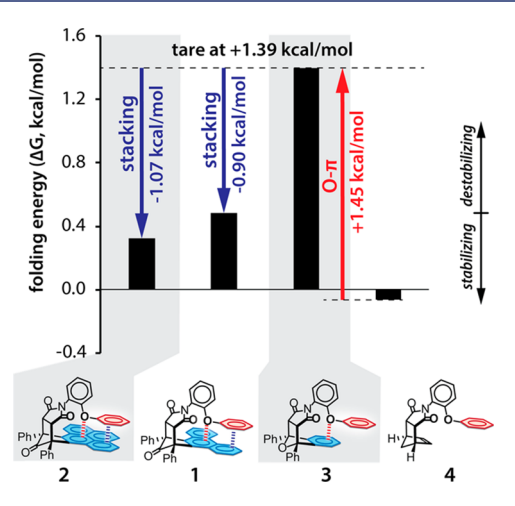


Figure 3. Folding energies of balances 1 and 2 measure the attractive stacking interactions (blue broken lines) and control balances 3 and 4 to isolate the repulsive $O-\pi$ interactions (red broken lines) in CDCl₃ at 25 °C. Data are from ref 1.

system as the folding ratio was very close to unity upon removing this repulsive interaction.

Another appealing characteristic of the N-arylimide balances was the ability to confirm the formation and characterize the distances and geometry of the intermolecular interactions via X-ray crystal structures. Most balances readily yielded X-ray-quality crystals of the folded conformation through slow evaporation from organic solvents, especially if the folded conformation was the thermodynamically more stable conformer in solution. For example, the arm and shelf units in balances $\mathbf{5-7}$ formed well-defined offset stacking, carbonyl $-\pi$, and CH $-\pi$ interactions, respectively, in the solid state (Figure 4). A-21,22 The X-ray crystal structures not only confirmed the design and function of the molecular balances but also helped

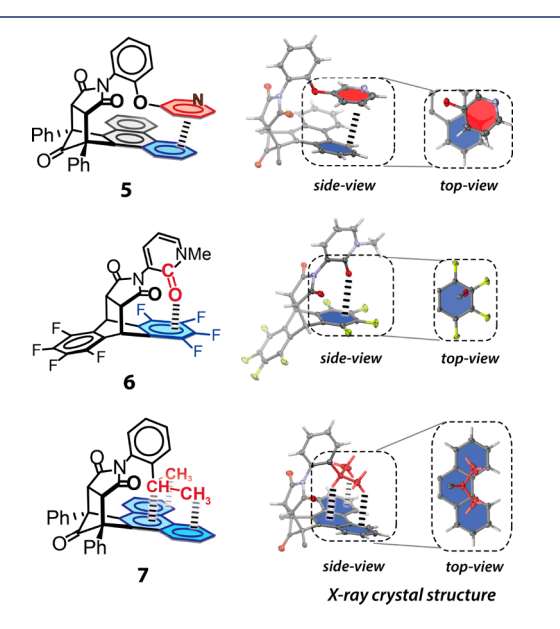


Figure 4. Side- and top-views of the X-ray crystal structures of balances **5**, **6** and **7** highlighting the formation of intramolecular heterocyclic— π , carbonyl— π , and CH— π interactions between the arm (red) and aromatic shelf (blue) units. The bridgehead phenyl groups in **5** and **7** were omitted for visual clarity in the X-ray structures. Data are from refs **4**, 20, and 21.

elucidate the observed aromatic interaction trends. For example, the enhanced stability of the heterocycle— π stacking interaction in balance 5 was attributed to the electrostatic complementarity of the polar heterocyclic ring with the aromatic shelf (vide infra).²¹ The strong CH— π interaction in balance 7, on the other hand, was attributed to the formation of multiple close contacts between the branched *iso*-propyl arm and phenanthrene shelf, enhancing dispersion and solvophobic effects.²²

■ IMPACT AND UTILITY

At the outset of our studies, we did not fully appreciate the importance and challenges associated with measuring aromatic interactions. We assumed that aromatic interactions were well understood as their ubiquity and importance in biological and synthetic systems had been widely recognized. Therefore, we were surprised by the very positive feedback from our first set of publications and the encouragement from theoretical chemists to carry out more studies as there was a deficit of good experimental data to assist in improving computational models.

Studies of aromatic interactions face a number of unique challenges. First, aromatic interactions, unlike hydrogen bonding or ion pairing, are not solely dominated by electrostatics.²³ Aromatic interactions have significant contributions from electrostatics, steric repulsion, dispersion,² and solvent effects, ^{19,25} which all have to be taken into consideration when predicting their interaction energies or stability trends. 10,26 Furthermore, the relative contributions of these components can change in the course of a study as the geometry, structure, or environment is systematically altered.²⁷ Second, many aromatic interactions have relatively flat potential energy surfaces due to the absence of a dominant electrostatic component. ²⁸ The interacting surfaces can adopt an array of geometries with similar interaction energies. For example, the arene-arene interaction can adopt a number of distinct geometries with similar interaction energies such as edge-to-face (monodentate and bidentate), tilted, and offset stacking.²⁹ Thus, the most stable geometry can vary from system to system. Finally, accurately predicting the dispersion and solvent effects of aromatic interactions is still very challenging. The simulation of dispersion interactions has only recently become widely accessible using either high-level electron-electron correlation methods³⁰ or calibrated dispersion corrections.³¹ Similarly, the modeling of solvent effects is still a field of active research as accurate simulations of explicit solvent molecules remain computationally expensive and hybrid/combined quantum-mechanical models are still in development.32-3

■ SYNTHETIC ACCESSIBILITY AND VERSATILITY

Synthetic efficiency and versatility were also critical elements in the success of the N-arylimide balances. The modular and convergent synthesis was important as each interacting surface had to be covalently attached to the balance framework, and multiple balances were required to measure each interaction. The balances were assembled via two high-yielding reactions (Figure 5). (1) A condensation reaction between a cyclic anhydride and an ortho-substituted aniline forms the key rotating C_{aryl} – N_{imide} bond. (2) A Diels–Alder reaction between a diene and maleic anhydride (or maleimide) dienophile constructs the rigid C-shaped framework. Neither

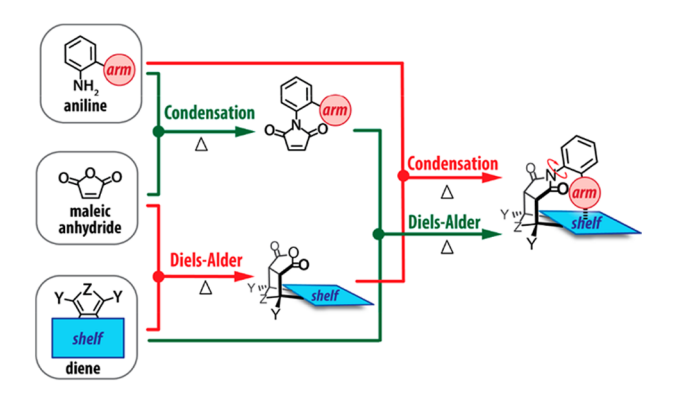


Figure 5. Representation of the convergent synthesis of the *N*-arylimide molecular balances.

key step requires additional reagents or catalysts; simply heating the components in solution or neat yielded the desired products. The order of the key steps can be varied depending on the availability of the starting materials and the efficiency of the final step.

The synthetic versatility also enabled the rapid production of balances with varying arm and shelf units to study a wide range of interactions (Figure 6). Libraries of dienes containing different aromatic shelves were combined with libraries of anilines containing different arm units. Thus, N-arylimide molecular balances were prepared to study an array of aromatic interactions, including aromatic stacking 1,35 and heterocycle- π , 21 cation- π , 21 substituent- π , 23 CH/D- π , 17,22,36,37

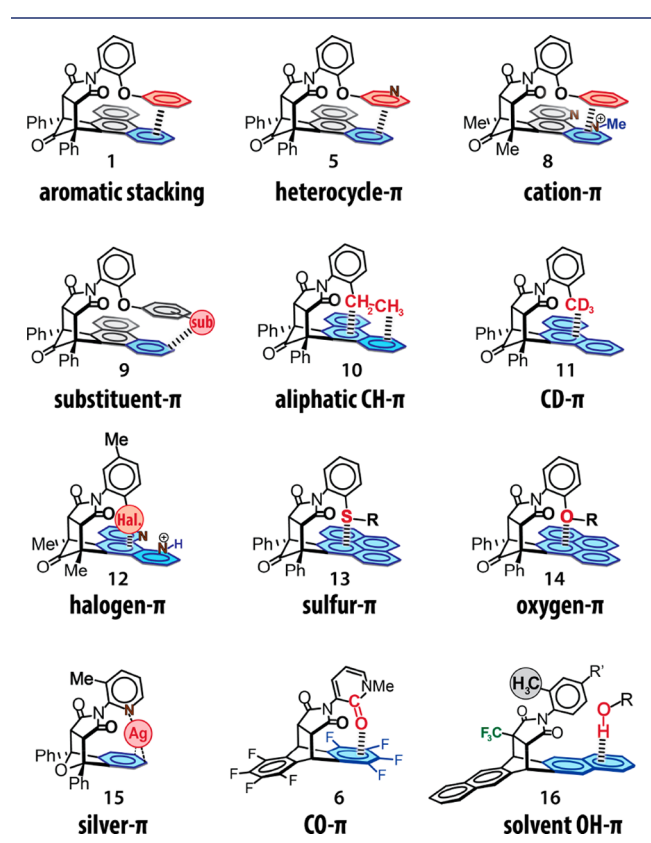


Figure 6. Examples of *N*-arylimide balances highlighting the many types of noncovalent aromatic interactions that can be formed and studied.

halogen $-\pi$, ^{4,38} sulfur $-\pi$, ³⁹ oxygen $-\pi$, ^{4,39} and silver $-\pi$, ⁴⁰ CO $-\pi$, ⁴ and solvent OH $-\pi$ ⁴¹ interactions.

TESTING HYPOTHESES AND ANSWERING OUESTIONS

The most exciting aspect of our balance studies was being able to address fundamental questions and to test hypotheses about the nature and origins of aromatic interactions. The answers were often surprising and contrary to our expectations, or I (K.D.S.) should clarify that the results were contrary to my expectations. At some point, my research group took it as a challenge to disprove my predictions as each time they were successful it would inevitably lead to a publication in a top journal. We investigated many new aromatic interactions that I was initially very skeptical of, such as sulfur— π , fluorine— π , and carbonyl— π interactions. In most cases, we were able to observe and measure the new interactions and demonstrate that they were stabilizing for specific structures or environments.

An example of our ability to test hypotheses was our contributions to examining the origins of the aromatic stacking substituent effects (SEs). The ability of substituents to influence the strength of stacking interactions has long been recognized, 42,43 with electron-withdrawing groups generally strengthening the interaction. An intriguing hypothesis was advanced by Wheeler and Houk in 2009 that the SEs were due to the direct interactions of the substituents with the aromatic surface and not through the polarization of the attached aromatic ring.44 A consequence of this through-space hypothesis is that each substituent would act independently, and thus their effects would be additive, which was something that we could test using our molecular balances. A series of 20 stacking balance systems containing 1, 2, or 3 electrondonating (OCH3 and CH3) or -withdrawing (CN, Cl, and NO₂) substituents were synthesized, and their folding ratios were measured in solution.² The SEs for balances with multiple substituents were almost perfectly additive as predicted by the Wheeler-Houk model. For example, the measured SE for a single meta-CH₃ group was -0.19 kcal/mol. Therefore, m,m'diCH₃ groups had a predicted additive substituent effect of -0.38 kcal/mol (-0.19 + -0.19 kcal/mol) which was very close to the measured value of -0.35 kcal/mol (Figure 7).

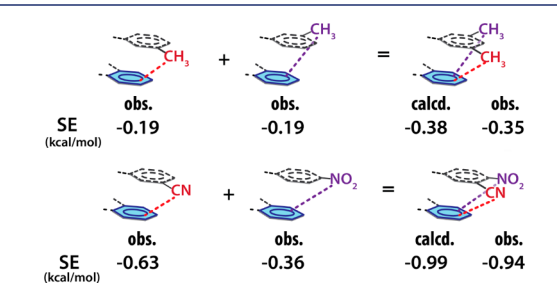


Figure 7. Observed and calculated additivity of substituent effects (SEs) in multisubstituted aromatic stacking balance 9 in CDCl₃. Data are from ref 2.

Similar additive trends were observed for electron-withdrawing (Figure 7, meta-CN + para-NO₂) and electron-donating groups and combinations of the two. The additivity of the substituent effects supports the Wheeler–Houk through-space model providing a simple predictive model for developing and

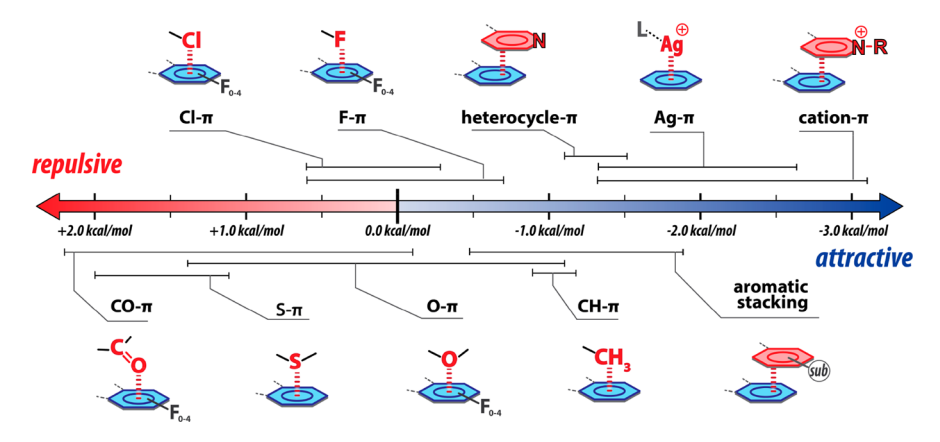


Figure 8. Comparison of the interaction strengths of aromatic interactions between various functional groups and benzenoid surfaces measured using our *N*-arylimide molecular balances in CDCl₃. (See the SI for details.) The interacting units for each interaction type are highlighted.

optimizing pharmaceuticals, supramolecular structures, and catalysts that utilize stacking interactions.

Examples of the questions addressed using the *N*-arylimide balances are listed below:

Q: Are $CD-\pi$ interactions stronger than $CH-\pi$ interactions?

A: In our balances, the strengths of the $CD-\pi$ and $CH-\pi$ interactions were identical within experimental error, which was consistent with high-level calculations. We hypothesized that the isotope effects observed in previous systems may be due to their greater rigidity, which distinguished the C-D and C-H bond lengths.³⁶

Q: Are $S-\pi$ interactions more stabilizing than $O-\pi$ interactions?

A: The relative stability of $S-\pi$ versus $O-\pi$ was dependent on the structural, geometric, and solvent parameters. At shorter distances, the $O-\pi$ interaction was lower in energy due to the greater sterics of the larger sulfur atoms. At longer distances, the $S-\pi$ interaction was lower in energy, presumably due to the greater contact surface area of the larger sulfur atoms. ³⁹

Q: Can we observe the increase in the dispersion component of aromatic stacking interactions in organic solution by increasing the size of the aromatic surface?

A: When the surface contact area of the stacking interaction was kept constant but the overall size of the surface was increased, we were unable to observe any changes. This could be due to the small changes in polarizability between aromatic surfaces and/or the dispersion contributions to the stacking interactions in organic solvents being smaller than the sensitivity of our balances.³⁵

Q: Do polarized alkyl groups connected to electronegative groups form any additional interactions with polar aromatic surfaces?

A: Alkyl groups attached to electronegative oxygen such as in ethers and esters can form additional aromatic interactions via the bond dipole of the polarized C–O bond. These polarized alkyl groups, for instance, can interact with the dipoles of heterocyclic surfaces, forming more stabilizing and attractive interactions when the dipoles are favorably oriented.³⁷

Q: Do the conformer ratios in solution match the conformational preferences in the crystal structures of atropisomeric systems when the differences due to packing effects are minimized?

A: There was a correlation between the solution and solid-state folding ratios. However, the correlation was not linear but a step function. If a balance significantly preferred a conformer in solution, then the crystal structure was usually 100% of the favored conformer. However, if the folding ratio in solution was close to unity ($K_{\rm eq}=1.0\pm0.24$), then the crystal structure would often be a mixture of folded and unfolded conformers and the ratios could be anywhere from fully folded to fully unfolded.²⁰

■ ELECTROSTATIC TRENDS

The versatility of the *N*-arylimide balances provided the unique opportunity to directly compare the interaction strengths of a wide array of aromatic interactions within the same system and to identify general trends. Thus, we could answer the following practical question: if you are designing a system that relies on these interactions, what structural changes would lead to the largest increase or decrease in stability? Figure 8 compares the interaction strengths of some of the more common aromatic interactions studied using our balances. The most attractive interactions were pyridinium cation- π and silver- π interactions. Neutral groups also formed stabilizing but weaker interactions with aromatic surfaces in solution. These included aromatic groups that formed stacking interactions and alkyl groups that formed CH $-\pi$ interactions. Arm units containing electronegative atoms such as halogens and chalcogens generally formed destabilizing interactions with aromatic surfaces. However, the interaction energies varied widely depending on the charge and substituents on the aromatic surface and in some cases could become attractive.

Several general trends stood out. First, the strongest attractive and repulsive interactions were aromatic interactions that had larger than normal electrostatic terms. Aromatic surfaces are generally considered to be nonpolar. However, even unsubstituted aromatic surfaces contain distinct electrostatic positive and negative regions. The aromatic quadrupole has a negative π -face and a positive edge as exemplified by the quadrupole of benzene (Figure 9, left). Thus, the strongest interactions involve groups with positive charges such as pyridinium and silver(I) ions that can form attractive electrostatic interactions with the partially electronically negative π -face of the aromatic surface. The metal $-\pi$ interaction of the silver(I) ion had interaction strengths of -1.3 to -2.6 kcal/mol depending on the geometry of the interaction and the ligands on the silver. The pyridinium

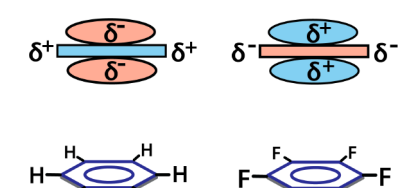


Figure 9. Schematic illustration of the electrostatic charge distributions (top structures) of benzene and hexafluorobenzene (bottom structures) arising from their quadrupoles.

cations also formed strong attractive stacking interactions with aromatic surfaces of up to $-3.1 \text{ kcal/mol.}^{21}$ The enhanced strength of the cation—aromatic interactions helps to explain and validate Stoddart's design choice of pyridinium units in his rotaxane and pseudorotaxane systems that required strong stacking interactions for their synthesis and function. 45,46

The geometric variations in the pyridinium—aromatic stacking interaction strengths provided further support for the ability of complementary electrostatic interactions to strengthen aromatic interactions (Figure 10).²¹ Balance 19 that

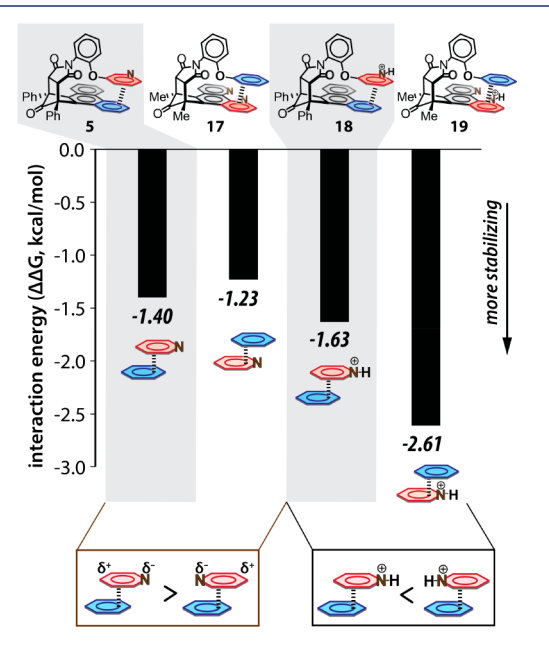


Figure 10. Relative interaction energies for the stacking interactions of six-membered benzene, pyridine, and pyridinium rings measured using our molecular balances in DMSO- d_6 at 25 °C. Data are from ref 21.

positioned the pyridinium nitrogen over the aromatic surface formed the strongest interaction as it aligned the positive charge with the complementary partial negative face of the aromatic surface. Conversely, when the positive nitrogen was over the edge of the aromatic surface (balance 18), the interaction was much weaker due to its proximity to the electrostatically similar positive hydrogens on the edge of the aromatic shelf.

The opposite trends were observed for the stacking interactions of neutral heterocycles (balances 5 and 17). However, the trends were still consistent with the electrostatic picture of the stacking interaction. The more stable geometry had the neutral nitrogen over the edge (balance 5) as opposed to over the face of the aromatic ring (balance 17). The neutral

nitrogen is more electronegative than carbon and thus carries a partial negative charge which is complementary to the partial positive charge of the hydrogens on the edge of the aromatic surface. The geometric preferences of the neutral heterocycles were much smaller than those for the cationic pyridinium surfaces, as the partial charge on the neutral nitrogen formed weaker electrostatic interactions than a full positive charge.

DISPERSION AND SOLVOPHOBIC EFFECTS

The second general trend was the correlation between the surface area contact of the arm and shelf units and the strength of the aromatic interaction. This trend is well established in aqueous environments and in vacuo. However, the observation of the analogous trends in organic solvents was surprising, where solvophobic effects and dispersion interactions are considerably weaker. Thus, we were initially surprised to observe and measure the attractive interactions of nonpolar units with aromatic surfaces in organic solvents.³ For example, the nonpolar substituents of increasing size (i.e., iso-propyl and tert-butyl) at the para position of balance 9 formed increasingly stronger attractive interactions with the edge of the phenanthrene shelf in chloroform (Figure 11A, blue diamonds). The observation was contrary to the expected steric trends and echoed the stabilizing role of dispersion interaction bulky akanes. 47,48 We were not alone in observing and studying the interactions of nonpolar surfaces in organic solvents. Chen and co-workers recently confirmed that dispersion interactions still have a measurable impact on organic solvents such as methylene chloride despite the competition from solvent molecules. 49 Cockroft and coworkers demonstrated that these attractive interactions also have a significant solvophobic effect even in organic solvents, as demonstrated by their correlation with solvent cohesion (ced). 50 The precise nature of the attractive interactions of nonpolar surfaces in organic solvents is still being debated as both dispersion and solvophobic effects should show similar trends of increasing strength with increasing surface area contact. 51,52

Interestingly, the opposite trend was observed when the same alkyl substituents were at the closer meta position (Figure 11A, red squares). At these shorter distances, the originally expected steric trends were observed, where the smallest methyl group was the most stable and the largest tertbutyl group was the least stable. While the trends in the meta and para positions would seem to be at odds with each other, an analysis of the change in the solvent-accessible surface area (Δ SASA) for the para- and meta-substituted balances and additional multisubstituted balances demonstrated that they were governed by the same underlying trends (Figure 11B). An excellent correlation was observed between Δ SASA and the interaction energy which spanned interaction energies from attractive to repulsive.

■ ATTRACTION OF ELECTRON-RICH GROUPS

One of the most surprising trends that we observed was the ability of electronegative atoms such as ether oxygens, carbonyl oxygens, and even fluorines to form stabilizing aromatic interactions under specific conditions. As expected, arm units containing these atoms usually formed destabilizing interactions due to the electrostatic repulsion of the partial negative charge of these electronegative atoms with the partial negative charge of the π -face of the aromatic surface. However,

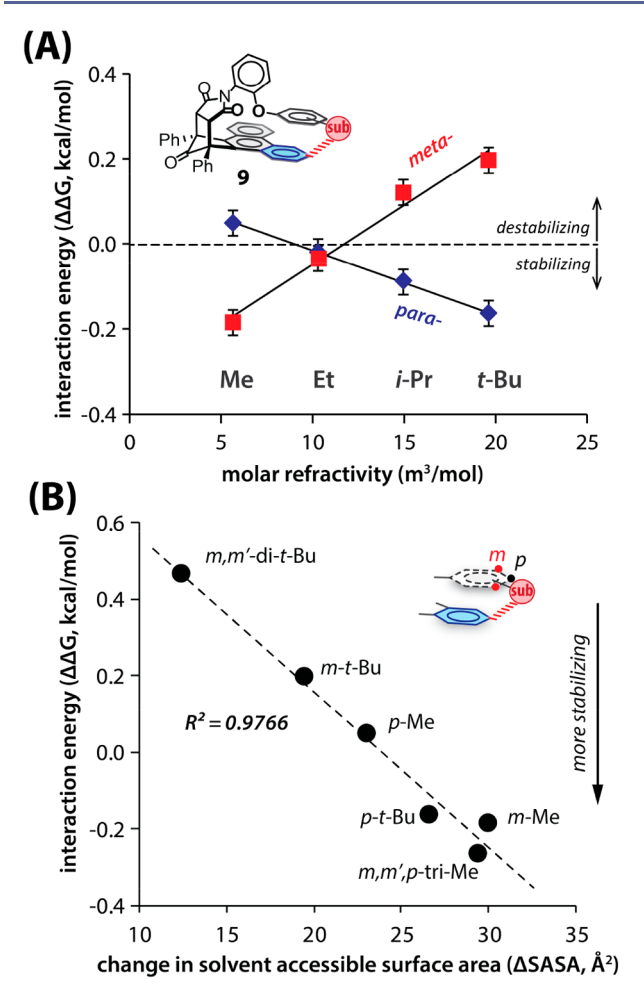


Figure 11. (A) Correlation of the substituent effects $(\Delta\Delta G)$ of *meta*-and *para*-alkyl substituents of varying size in balance 9 with the molar refractivity, a molecular descriptor closely correlated with the vdw volumes of alkyl groups. (Left to right) Methyl, ethyl, *iso*-propyl, and *tert*-butyl. (B) Measured interaction energy $(\Delta\Delta G)$ of nonpolar alkyl substituents in balance 9 correlated with the calculated change in the solvent-exposed surface area $(\Delta SASA)$ of the arm and shelf surfaces upon interaction in CDCl₃. Reproduced with permission from ref 3. Copyright 2016 Wiley.

the electrostatically negative π -face of an aromatic surface can be attenuated and even inverted to an electrostatically positive surface by the incorporation of multiple strong electronwithdrawing substituents (Figure 9, right) or the use of a heterocyclic or positively charged aromatic surface.³⁸ Thus, balances 7, 22, and 24 with electron-poor tetrafluoro aromatic shelves (Figure 12) can form stabilizing carbonyl $-\pi$, F $-\pi$, and $O-\pi$ interactions in comparison to their nonfluorinated control balances (20, 21, and 23).4 These attractive electrostatic interactions of the carbonyl, ether, and fluorine groups contrast with the behavior of methyl balances 25 and 26 that form nonpolar CH $-\pi$ interactions, which showed only a small difference in folding energy between the fluorinated and nonfluorinated shelves. While close contacts between electrostatically negative groups and π -surfaces are commonly observed in biological and solid-state structures, 53,54 the Narylimide balances provided some of the first experimental confirmations of their attractive nature and the magnitudes of their interaction energies.

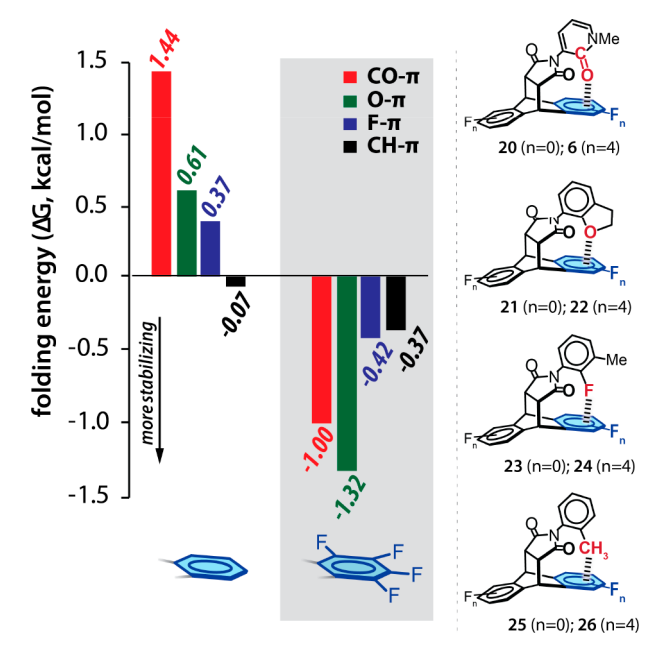


Figure 12. Folding energies for $CO-\pi$, $O-\pi$, $F-\pi$, and $CH-\pi$ balances in solution (CD_3CN) highlighting the change from repulsion for the unsubstituted aromatic shelf to attraction for the tetrafluoro aromatic shelf. Data are from ref 4.

■ SOLVENT EFFECTS

Another advantage of molecular balances is the intramolecular nature of the interactions, which enabled their consistent formation and study in a range of different solvent systems. 1,4,37,38,41,55 Although the solvent data were complex and difficult to model, a few trends did emerge. We and others observed the solvophobic effects in different organic solvents via the correlation of the interaction energies with the solvent cohesive energy density (ced). However, there was still considerable scatter in the correlation plots, suggesting that there are other significant contributing factors. By keeping the structures of the interacting surfaces constant, we were able to observe specific solvent—solute interactions such as the ability of protic solvents to form hydrogen-bonding interactions with the π -face 41 and anion effects in organic solvents. 55

We designed balance 16 (Figure 13) to study the solvent effects on the folding equilibrium. The balance had a nonpolar methyl arm that formed an intramolecular $CH-\pi$ interaction in the folded conformer and was soluble in a range of solvent systems from benzene and diethyl ether to DMSO and water. Consistent with the reports from the Cockroft group, 56,57 a solvophobic effect was observed as the folding energy $(-\Delta G)$ was strongly correlated with the solvent cohesion parameter, ced. Interestingly, separate trendlines were observed for the protic (red circles) and aprotic (blue circles) solvents. Contrary to our expectations, the protic solvents, which form strong solvent-solvent hydrogen-bonding interactions, had systematically smaller solvophobic effects than the aprotic solvents as seen by the smaller slope of the protic solvent trendline (Figure 13). We attributed these differences to the ability of protic solvents to form $OH-\pi$ interactions with the face of the aromatic shelf in the unfolded conformer, which attenuates the stronger solvent cohesion of protic solvents that would normally drive stronger solvophobic effects. The solvent $OH-\pi$ interactions have been previously observed in biological systems and to explain the solubility of aromatic

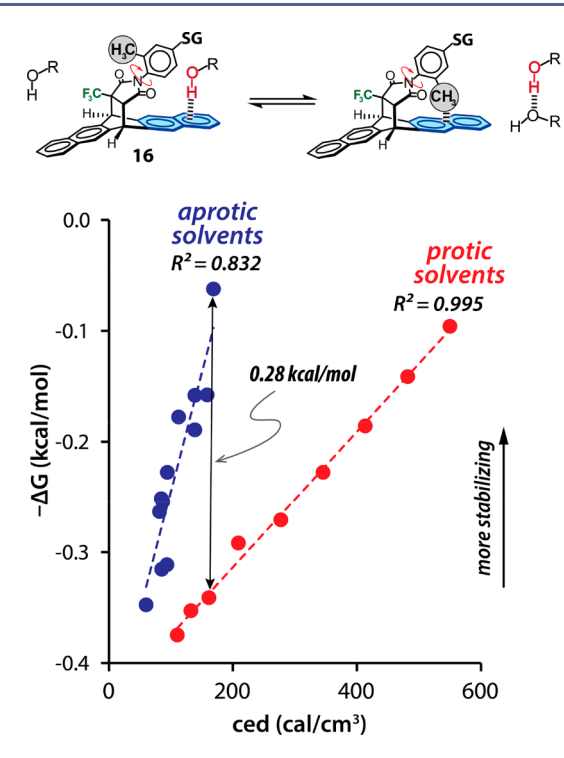


Figure 13. Correlation of solvophobic effects with solvent cohesion density (ced) across 19 solvent systems measured using a $\text{CH}-\pi$ molecular balance highlighting the different trends for protic and aprotic solvents. A solubilizing group (SG) of mono- or tetra-carboxylic acids was used to enhance the solubility in polar solvents. Data are from ref 41.

surfaces in protic solvents, especially water. However, the solvation of *ortho*-aromatic CH group might also have played a role in the higher folding energy $(-\Delta G)$ in aprotic solvents with greater hydrogen bond acceptor ability, especially in the presence of an electron-withdrawing carboxylic acid group at the meta position. ⁵⁸

SUMMARY AND OUTLOOK

What seemed at first like a simple solved problem proved to be a complex, engaging, and fulfilling journey. Like other good research tools, the N-arylimide balances provided answers, led inquiries in unanticipated directions, and raised even more questions about aromatic interactions. These molecular-scale instruments enabled the study of weak noncovalent interactions and provided insight into their nature and origins. The results have led to improvements in modeling and predictions of their strengths, geometries, and stability trends. 59,60 Key design attributes of the N-arylimide balances include synthesis versatility, ease of use, and accuracy. These attractive characteristics have been recognized by other researchers in studies of solvent effects 58,61,62 and halogen- π^{63} and alkylfullerene interactions.⁶⁴ Future challenges involve improving our understanding and modeling of solvent effects, the entropy of solvation, the relative contributions of solvophobic and dispersion interactions in organic solvents, and the accuracy of the balances by assessing the steric and entropic effects imposed by their geometric constraints

ASSOCIATED CONTENT

Supporting Information

The Supporting Information is available free of charge at https://pubs.acs.org/doi/10.1021/acs.accounts.0c00519.

Additional data tables for Figure 8 (PDF)

AUTHOR INFORMATION

Corresponding Author

Ken D. Shimizu — Department of Chemistry and Biochemistry, University of South Carolina, Columbia, South Carolina 29208, United States; orcid.org/0000-0002-0229-6541; Email: shimizu@mailbox.sc.edu

Authors

Ping Li — Chemical Sciences Division, Oak Ridge National Laboratory, Oak Ridge, Tennessee 37831, United States;
orcid.org/0000-0001-9339-3111

Erik C. Vik – Vertex Pharmaceuticals, Boston, Massachusetts 02210, United States; orcid.org/0000-0003-1334-0293

Complete contact information is available at: https://pubs.acs.org/10.1021/acs.accounts.0c00519

Notes

The authors declare no competing financial interest.

Biographies

Ping Li was raised in Tianjin, China. He received his bachelor's degree (2006) from the East China University of Science and Technology (ECUST), where he did postgraduate work with Wei Wang on organocatalysis. He obtained his Ph.D. (2015) from the University of South Carolina (U.S.C.) with Ken D. Shimizu on assessments of solution-phase aromatic interactions and subsequently became a postdoctoral associate at U.S.C. (2016–2020) working on weak molecular interactions and biorenewable polymers. He currently is a postdoctoral associate at Oak Ridge National Laboratory working on new materials for ion separation.

Erik C. Vik grew up in East Islip, New York and graduated from the State University of New York at Oswego in 2014 with a B.S. in chemistry working with Fehmi Damkaci on copper-catalyzed C-O and C-N Ullman coupling. He later graduated from the University of South Carolina in 2019 with a Ph.D. in chemistry working with Ken D. Shimizu on measuring rates of isomerization and conformational populations using NMR and computational chemistry. Currently, he is a postdoctoral associate with Vertex Pharmaceuticals working on the discovery of RNA-binding small molecules.

Ken D. Shimizu was born in Sapporo, Japan and raised in Kingston, RI, USA. He received his B.A. (1990) from Cornell University working with Jean M. Fréchet and his Ph.D. from the Massachusett Institute of Technology (1995) working with Julius Rebek and was an NIH postdoctoral fellow with Amir Hoveyda at Boston College. He joined the faculty at the University of South Carolina in 1997 and is currently a professor and the Department Chair. His research interests include molecular devices, the study of noncovalent interactions, and polymers with recognition properties.

ACKNOWLEDGMENTS

Funding for this work was provided by the National Science Foundation (grants CHE 1709086 and 2003889).

REFERENCES

- (1) Carroll, W. R.; Pellechia, P.; Shimizu, K. D. A Rigid Molecular Balance for Measuring Face-to-Face Arene-Arene Interactions. *Org. Lett.* **2008**, *10*, 3547–3550.
- (2) Hwang, J.; Li, P.; Carroll, W. R.; Smith, M. D.; Pellechia, P. J.; Shimizu, K. D. Additivity of Substituent Effects in Aromatic Stacking Interactions. *J. Am. Chem. Soc.* **2014**, *136*, 14060–14067.
- (3) Hwang, J.; Li, P.; Smith, M. D.; Shimizu, K. D. Distance-Dependent Attractive and Repulsive Interactions of Bulky Alkyl Groups. *Angew. Chem., Int. Ed.* **2016**, *55*, 8086–8089.
- (4) Li, P.; Vik, E. C.; Maier, J. M.; Karki, I.; Strickland, S. M. S.; Umana, J. M.; Smith, M. D.; Pellechia, P. J.; Shimizu, K. D. Electrostatically Driven CO- π Aromatic Interactions. *J. Am. Chem. Soc.* **2019**, *141*, 12513–12517.
- (5) Meyer, E. A.; Castellano, R. K.; Diederich, F. Interactions with Aromatic Rings in Chemical and Biological Recognition. *Angew. Chem., Int. Ed.* **2003**, *42*, 1210–1250.
- (6) Salonen, L. M.; Ellermann, M.; Diederich, F. Aromatic Rings in Chemical and Biological Recognition: Energetics and Structures. *Angew. Chem., Int. Ed.* **2011**, *50*, 4808–4842.
- (7) Neel, A. J.; Hilton, M. J.; Sigman, M. S.; Toste, F. D. Exploiting Non-Covalent π Interactions for Catalyst Design. *Nature* **2017**, *543*, 637–646
- (8) Waters, M. L. Aromatic Interactions. Acc. Chem. Res. 2013, 46, 873–873.
- (9) Mati, I. K.; Cockroft, S. L. Molecular Balances for Quantifying Non-Covalent Interactions. *Chem. Soc. Rev.* **2010**, *39*, 4195–4205.
- (10) Shimizu, K. D.; Li, P.; Hwang, J. Aromatic Interactions: Frontiers in Knowledge and Application; The Royal Society of Chemistry: 2017; Chapter 5, pp 124–171.
- (11) Oki, M. 1,9-Disubstituted Triptycenes an Excellent Probe for Weak Molecular-Interactions. *Acc. Chem. Res.* **1990**, 23, 351–356.
- (12) Paliwal, S.; Geib, S.; Wilcox, C. S. Molecular Torsion Balance for Weak Molecular Recognition Forces. Effects of "Tilted-T" Edgeto-Face Aromatic Interactions on Conformational Selection and Solid-State Structure. *J. Am. Chem. Soc.* **1994**, *116*, 4497–4498.
- (13) Aliev, A. E.; Motherwell, W. B. Some Recent Advances in the Design and Use of Molecular Balances for the Experimental Quantification of Intramolecular Noncovalent Interactions of π Systems. *Chem. Eur. J.* **2019**, 25, 10516–10530.
- (14) Verma, S. M.; Singh, N. B. A Study of Conformation About Aryl C-N Bonds in N-Aryl Imides by Dynamic NMR Spectroscopy. *Aust. J. Chem.* **1976**, *29*, 295–300.
- (15) Kishikawa, K.; Yoshizaki, K.; Kohmoto, S.; Yamamoto, M.; Yamaguchi, K.; Yamada, K. Control of the Rotational Barrier and Spatial Disposition of the N-(2'-Methylphenyl) Group in Succinimides by Substituent and Solvent Effects. *J. Chem. Soc., Perkin Trans.* 1 1997, 1233–1239.
- (16) Grossmann, G.; Potrzebowski, M. J.; Olejniczak, S.; Ziolkowska, N. E.; Bujacz, G. D.; Ciesielski, W.; Prezdo, W.; Nazarov, V.; Golovko, V. Structural Studies of N-(2 '-Substituted Phenyl)-9,10-Dihydro-9,10-Ethanoanthracene-11,12-Dicarboximides by X-Ray Diffraction and NMR Spectroscopy Proofs for CH/pi Interactions in Liquid and Solid Phases. *New J. Chem.* **2003**, 27, 1095–1101.
- (17) Carroll, W. R.; Zhao, C.; Smith, M. D.; Pellechia, P. J.; Shimizu, K. D. A Molecular Balance for Measuring Aliphatic $CH-\pi$ Interactions. *Org. Lett.* **2011**, *13*, 4320–4323.
- (18) Gung, B. W.; Xue, X.; Reich, H. J. The Strength of Parallel-Displaced Arene-Arene Interactions in Chloroform. *J. Org. Chem.* **2005**, *70*, 3641–3644.
- (19) Cubberley, M. S.; Iverson, B. L. H-1 NMR Investigation of Solvent Effects in Aromatic Stacking Interactions. *J. Am. Chem. Soc.* **2001**, *123*, 7560–7563.
- (20) Li, P.; Hwang, J.; Maier, J. M.; Zhao, C.; Kaborda, D. V.; Smith, M. D.; Pellechia, P. J.; Shimizu, K. D. Correlation between Solid-State and Solution Conformational Ratios in a Series of N-(o-Tolyl)-Succinimide Molecular Rotors. *Cryst. Growth Des.* **2015**, *15*, 3561–3564.

- (21) Li, P.; Zhao, C.; Smith, M. D.; Shimizu, K. D. Comprehensive Experimental Study of N-Heterocyclic π -Stacking Interactions of Neutral and Cationic Pyridines. *J. Org. Chem.* **2013**, *78*, 5303–5313.
- (22) Zhao, C.; Li, P.; Smith, M. D.; Pellechia, P. J.; Shimizu, K. D. Experimental Study of the Cooperativity of CH- π Interactions. *Org. Lett.* **2014**, *16*, 3520–3523.
- (23) Anslyn, E. V.; Dougherty, D. A. Modern Physical Organic Chemistry; University Science: Sausalito, CA, 2006.
- (24) Sherrill, C. D. Energy Component Analysis of π Interactions. *Acc. Chem. Res.* **2013**, *46*, 1020–1028.
- (25) Hunter, C. A. Quantifying Intermolecular Interactions: Guidelines for the Molecular Recognition Toolbox. *Angew. Chem., Int. Ed.* **2004**, *43*, 5310–5324.
- (26) Hwang, J.; Li, P.; Shimizu, K. D. Synergy between Experimental and Computational Studies of Aromatic Stacking Interactions. *Org. Biomol. Chem.* **2017**, *15*, 1554–1564.
- (27) Arnstein, S. A.; Sherrill, C. D. Substituent Effects in Parallel-Displaced π - π Interactions. *Phys. Chem. Chem. Phys.* **2008**, 10, 2646–2655
- (28) Sinnokrot, M. O.; Sherrill, C. D. Highly Accurate Coupled Cluster Potential Energy Curves for the Benzene Dimer: Sandwich, T-Shaped, and Parallel-Displaced Configurations. *J. Phys. Chem. A* **2004**, *108*, 10200–10207.
- (29) Tsuzuki, S.; Uchimaru, T.; Sugawara, K.; Mikami, M. Energy Profile of the Interconversion Path Between T-shape and Slipped-parallel Benzene Dimers. *J. Chem. Phys.* **2002**, *117*, 11216–11221.
- (30) Hohenstein, E. G.; Sherrill, C. D. Wavefunction Methods for Noncovalent Interactions. Wiley Interdisciplinary Reviews: Computational Molecular Science 2012, 2, 304–326.
- (31) Grimme, S. Density Functional Theory with London Dispersion Corrections. Wiley Interdiscip. Rev.: Comput. Mol. Sci. 2011, 1, 211–228.
- (32) Friesner, R. A.; Guallar, V. Ab Initio Quantum Chemical and Mixed Quantum Mechanics/Molecular Mechanics (QM/MM) Methods for Studying Enzymatic Catalysis. *Annu. Rev. Phys. Chem.* **2005**, *56*, 389–427.
- (33) Tomasi, J.; Mennucci, B.; Cammi, R. Quantum Mechanical Continuum Solvation Models. *Chem. Rev.* **2005**, *105*, 2999–3093.
- (34) Senn, H. M.; Thiel, W. QM/MM Methods for Biomolecular Systems. *Angew. Chem., Int. Ed.* **2009**, *48*, 1198–1229.
- (35) Hwang, J.; Dial, B. E.; Li, P.; Kozik, M. E.; Smith, M. D.; Shimizu, K. D. How Important Are Dispersion Interactions to the Strength of Aromatic Stacking Interactions in Solution? *Chem. Sci.* **2015**, *6*, 4358–4364.
- (36) Zhao, C.; Parrish, R. M.; Smith, M. D.; Pellechia, P. J.; Sherrill, C. D.; Shimizu, K. D. Do Deuteriums Form Stronger $CH-\pi$ Interactions? *J. Am. Chem. Soc.* **2012**, *134*, 14306–14309.
- (37) Li, P.; Parker, T. M.; Hwang, J.; Deng, F.; Smith, M. D.; Pellechia, P. J.; Sherrill, C. D.; Shimizu, K. D. The CH- π Interactions of Methyl Ethers as a Model for Carbohydrate-N-Heteroarene Interactions. *Org. Lett.* **2014**, *16*, 5064–5067.
- (38) Li, P.; Maier, J. M.; Vik, E. C.; Yehl, C. J.; Dial, B. E.; Rickher, A. E.; Smith, M. D.; Pellechia, P. J.; Shimizu, K. D. Stabilizing Fluorine- π Interactions. *Angew. Chem., Int. Ed.* **2017**, *56*, 7209–7212. (39) Hwang, J.; Li, P.; Smith, M. D.; Warden, C. E.; Sirianni, D. A.; Vik, E. C.; Maier, J. M.; Yehl, C. J.; Sherrill, C. D.; Shimizu, K. D. Tipping the Balance between S- π and O- π Interactions. *J. Am. Chem. Soc.* **2018**, *140*, 13301–13307.
- (40) Maier, J. M.; Li, P.; Hwang, J.; Smith, M. D.; Shimizu, K. D. Measurement of Silver– π Interactions in Solution Using Molecular Torsion Balances. *J. Am. Chem. Soc.* **2015**, *137*, 8014–8017.
- (41) Maier, J. M.; Li, P.; Vik, E. C.; Yehl, C. J.; Strickland, S. M. S.; Shimizu, K. D. Measurement of Solvent OH- π Interactions Using a Molecular Balance. *J. Am. Chem. Soc.* **2017**, *139*, 6550–6553.
- (42) Cockroft, S. L.; Hunter, C. A.; Lawson, K. R.; Perkins, J.; Urch, C. J. Electrostatic Control of Aromatic Stacking Interactions. *J. Am. Chem. Soc.* **2005**, 127, 8594–8595.
- (43) Cockroft, S. L.; Perkins, J.; Zonta, C.; Adams, H.; Spey, S. E.; Low, C. M. R.; Vinter, J. G.; Lawson, K. R.; Urch, C. J.; Hunter, C. A.

- Substituent Effects on Aromatic Stacking Interactions. Org. Biomol. Chem. 2007, 5, 1062–1080.
- (44) Wheeler, S. E.; Houk, K. N. Substituent Effects in the Benzene Dimer Are Due to Direct Interactions of the Substituents with the Unsubstituted Benzene. *J. Am. Chem. Soc.* **2008**, *130*, 10854–10855.
- (45) Pease, A. R.; Jeppesen, J. O.; Stoddart, J. F.; Luo, Y.; Collier, C. P.; Heath, J. R. Switching Devices Based on Interlocked Molecules. *Acc. Chem. Res.* **2001**, *34*, 433–444.
- (46) Barin, G.; Coskun, A.; Fouda, M. M. G.; Stoddart, J. F. Mechanically Interlocked Molecules Assembled by π - π Recognition. *ChemPlusChem* **2012**, *77*, 159–185.
- (47) Schreiner, P. R.; Chernish, L. V.; Gunchenko, P. A.; Tikhonchuk, E. Y.; Hausmann, H.; Serafin, M.; Schlecht, S.; Dahl, J. E. P.; Carlson, R. M. K.; Fokin, A. A. Overcoming lability of extremely long alkane carbon-carbon bonds through dispersion forces. *Nature* **2011**, *477*, 308–311.
- (48) Wagner, J. P.; Schreiner, P. R. London Dispersion in Molecular Chemistry—Reconsidering Steric Effects. *Angew. Chem., Int. Ed.* **2015**, *54*, 12274–12296.
- (49) Pollice, R.; Bot, M.; Kobylianskii, I. J.; Shenderovich, I.; Chen, P. Attenuation of London Dispersion in Dichloromethane Solutions. *J. Am. Chem. Soc.* **2017**, *139*, 13126–13140.
- (50) Yang, L.; Adam, C.; Nichol, G. S.; Cockroft, S. L. How Much Do van Der Waals Dispersion Forces Contribute to Molecular Recognition in Solution? *Nat. Chem.* **2013**, *5*, 1006–1010.
- (51) Ehrlich, S.; Moellmann, J.; Grimme, S. Dispersion-Corrected Density Functional Theory for Aromatic Interactions in Complex Systems. *Acc. Chem. Res.* **2013**, *46*, 916–926.
- (52) Schneider, H.-J. Dispersive Interactions in Solution Complexes. *Acc. Chem. Res.* **2015**, *48*, 1815–22.
- (53) Egli, M.; Sarkhel, S. Lone Pair-Aromatic Interactions: To Stabilize or Not to Stabilize. *Acc. Chem. Res.* **2007**, *40*, 197–205.
- (54) Mooibroek, T. J.; Gamez, P.; Reedijk, J. Lone Pair-π Interactions: a New Supramolecular Bond? *CrystEngComm* **2008**, *10*, 1501–1515.
- (55) Maier, J. M.; Li, P.; Ritchey, J. S.; Yehl, C. J.; Shimizu, K. D. Anion-Enhanced Solvophobic Effects in Organic Solvent. *Chem. Commun.* **2018**, *54*, 8502–8505.
- (56) Yang, L.; Adam, C.; Cockroft, S. L. Quantifying Solvophobic Effects in Nonpolar Cohesive Interactions. *J. Am. Chem. Soc.* **2015**, 137, 10084–10087.
- (57) Adam, C.; Yang, L.; Cockroft, S. L. Partitioning Solvophobic and Dispersion Forces in Alkyl and Perfluoroalkyl Cohesion. *Angew. Chem., Int. Ed.* **2015**, *54*, 1164–1167.
- (58) Emenike, B. U.; Spinelle, R. A.; Rosario, A.; Shinn, D. W.; Yoo, B. Solvent Modulation of Aromatic Substituent Effects in Molecular Balances Controlled by CH- π Interactions. *J. Phys. Chem. A* **2018**, 122, 909–915.
- (59) Nijamudheen, A.; Jose, D.; Shine, A.; Datta, A. Molecular Balances Based on Aliphatic CH- π and Lone-Pair- π Interactions. *J. Phys. Chem. Lett.* **2012**, *3*, 1493–1496.
- (60) Xie, M.; Lu, W. Attraction or Repulsion? Theoretical Assessment of Bulky Alkyl Groups by Employing Dispersion-Corrected DFT. RSC Adv. 2018, 8, 2240–2247.
- (61) Emenike, B. U.; Bey, S. N.; Bigelow, B. C.; Chakravartula, S. V. S. Quantitative Model for Rationalizing Solvent Effect in Noncovalent CH-Aryl Interactions. *Chem. Sci.* **2016**, *7*, 1401–1407.
- (62) Emenike, B. U.; Bey, S. N.; Spinelle, R. A.; Jones, J. T.; Yoo, B.; Zeller, M. Cationic CH-π Interactions as a Function of Solvation. *Phys. Chem. Chem. Phys.* **2016**, *18*, 30940–30945.
- (63) Sun, H.; Horatscheck, A.; Martos, V.; Bartetzko, M.; Uhrig, U.; Lentz, D.; Schmieder, P.; Nazare, M. Direct Experimental Evidence for Halogen-Aryl π Interactions in Solution from Molecular Torsion Balances. *Angew. Chem., Int. Ed.* **2017**, *56*, 6454–6458.
- (64) Yu, \dot{Y} . M.; Shi, L. J.; Yang, D. Z.; Gan, L. B. Molecular Containers with a Dynamic Orifice: Open-Cage Fullerenes Capable of Encapsulating Either H_2O or H_2 under Mild Conditions. *Chem. Sci.* **2013**, *4*, 814–818.